Title
Krypton in the Chassigny meteorite shows Mars accreted chondritic volatiles before nebular gases

Journal
Science, 377(6603)

ISSN
0036-8075 1095-9203

Authors
Péron, Sandrine
Mukhopadhyay, Sujoy

Publication Date
2022-07-15

DOI
10.1126/science.abk1175

Title: Krypton in the Chassigny meteorite shows Mars accreted chondritic volatiles before nebular gases

Authors: Sandrine Péron[1*]†, Sujoy Mukhopadhyay[1]

Affiliations:

[1]Department of Earth and Planetary Sciences, University of California – Davis, Davis, California 95616, United States of America

*Corresponding author. Email: sandrine.peron@erdw.ethz.ch

†Present address: Institute of Geochemistry and Petrology, ETH Zürich, 8092 Zürich, Switzerland

Abstract: Volatile elements are thought to have been delivered to Solar System terrestrial planets late in their formation, by accreting chondritic meteorites. Mars can provide information on inner Solar System volatile delivery during the earliest planet formation stages. We measured krypton isotopes in the Martian meteorite Chassigny, representative of the planet's interior. We find chondritic krypton isotope ratios, implying early incorporation of chondritic volatiles. Mars' atmosphere has different (solar-type) krypton isotope ratios, indicating it is not a product of magma ocean outgassing or fractionation of interior volatiles. Atmospheric krypton instead originates from accretion of solar nebula gas, after the mantle formed, but prior to nebular dissipation. Our observations contradict the common hypothesis that during planet formation, chondritic volatile delivery occurs after solar gas acquisition.

Main text:

Terrestrial planets acquire their volatile elements (e.g., hydrogen, carbon, nitrogen, noble gases) during formation. Models of this process often start with gases derived from the solar nebula (*1*), subsequently modified by fractionation during atmospheric escape and addition of volatiles from chondritic meteorites, either during the main accretionary phase (*2*–*4*), or as a late veneer towards the end stages of planet formation (*1*, *5*). The exact sources and timing of these events remain under debate (*2*–*7*). For example, capture of nebular volatiles by planets is not universally accepted as chondritic signatures are observed for most volatile elements (*2*, *5*–*7*). Potential chondritic contributions come from accretion of solid bodies originating from the inner Solar System with compositions similar to enstatite chondrite meteorites (*6*), or from the outer Solar System with compositions similar to carbonaceous chondrite meteorites or comets (*7*, *8*).

Due to their chemical inertness, noble gases retain a record of volatile accretion and the physical processes associated with it. In the Earth's mantle, helium and neon have solar-like isotope ratios; whereas the heavy noble gases (argon, krypton, xenon) have a chondritic origin (*2*, *4*, *9*, *10*). These observations can be interpreted as either simultaneous accretion of solar and chondritic volatiles, or early acquisition of solar volatiles followed by late addition of chondritic volatiles, provided the latter were mixed into the Earth's interior (*2*, *11*). As Mars mostly formed in the first 4 Myr of Solar System formation (*12*), it can provide information on volatile accretion during the earliest planet formation stages.

The Martian meteorite Chassigny has trapped noble gases (*13*) thought to represent Mars' interior composition (*14–16*). Analyses of xenon isotopes in Chassigny indicate Mars' mantle contains solar xenon (*14*, *15*), and by inference solar krypton (*16*). Xenon in Mars' atmosphere is mass-fractionated towards heavy isotopes, but consistent with an originally solar composition (*17*, *18*). Mars rover and Martian meteorite measurements show that the atmospheric krypton isotopic composition is indistinguishable from solar (*17*). Therefore, both the Martian mantle and atmosphere were argued to contain solar noble gases (*14–18*) with no indication of a chondritic contribution, potentially implying that Mars accreted all of its noble gases from the solar nebula.

However, xenon alone might not determine the sources of Mars' interior volatiles (*19*). The light isotopes (^{124}Xe, ^{126}Xe, ^{128}Xe, ^{130}Xe), stable and non-radiogenic, have nearly indistinguishable ratios for solar, chondritic and cometary sources. The solar isotope ratios for the heavier isotopes (^{131}Xe, ^{132}Xe, ^{134}Xe, ^{136}Xe) are intermediate between chondritic and cometary sources (*8*), and these isotopes are also produced during spontaneous fission of ^{244}Pu (now extinct) and ^{238}U (still extant) (*10*).

Krypton isotopes in Chassigny could potentially discriminate between solar and chondritic sources given their large isotopic differences: solar krypton is enriched in light isotopes (relative to Earth's atmosphere), while chondritic krypton is enriched in the heavier isotopes (*20*, *21*). However, previous krypton isotopic measurements of Chassigny had insufficient precision to distinguish between solar and chondritic sources (*14*, *16*, *22*). In addition, Chassigny was exposed to cosmic rays during transit to Earth (11 Myr exposure age) (*14*), producing cosmogenic krypton isotopes from spallation reactions, partially masking the signature of trapped krypton (*14*).

We measured noble gas abundances and isotope ratios for Ne, Ar, Kr, and Xe in two separate samples of Chassigny using laser step-heating (temperature steps between 280 °C and 1570 °C). We specifically developed a protocol for heavy noble gas separation and multi-collector noble gas mass spectrometry (*13*). The krypton and xenon isotope ratios in Chassigny are shown in Figures 1 and 2, respectively, numerical values are listed in Tables S1-S2, and additional isotope combinations are plotted in Figures S1-S3.

We find the krypton data fall on a single line, reflecting mixing of cosmogenic gases with trapped Martian mantle gases (Figs. 1, S1). Except ^{86}Kr, all Kr isotopes are produced via spallation reaction, with ^{83}Kr having the highest production rate (*13*). We therefore use the ^{86}Kr/^{84}Kr ratio to evaluate the source of Martian mantle heavy noble gases. By plotting ^{86}Kr/^{84}Kr as a function of ^{83}Kr/^{84}Kr, we determine the ^{86}Kr/^{84}Kr ratio corresponding to a ^{83}Kr/^{84}Kr value free of cosmogenic Kr; the result is the trapped mantle component (*13*).

Similarly, the xenon isotopic data fall on a mixing line (Figs. 2, S2) between cosmogenic and Martian mantle compositions. The first four temperature steps between 280 °C and 575 °C (Tables S1-S3) show a large contribution from Earth's air, with Ne, Ar, Kr and Xe isotopic ratios either close to Earth's air, or intermediate between air and the cosmogenic value (*13*). Because these are the initial low temperature steps, they likely represent shallow contamination of Chassigny by Earth's atmosphere (*15*). As the subsequent heating steps do not show signs of Earth air contamination for neon, argon, krypton or xenon, we use them to infer the Martian mantle composition. We discard the first four steps in our subsequent analysis and discussion.

Mars' interior ^{86}Kr/^{84}Kr ratio differs from the solar composition, but is indistinguishable from average carbonaceous chondrites (AVCC) (*13*). Fig. 1 shows that a mixture of solar and cosmogenic Kr does not pass through any of the measured data points, ruling out solar Kr as the trapped component. The krypton isotopic data do fall on a mixing line between a chondritic component and a cosmogenic component (*13*). Selecting the ^{83}Kr/^{84}Kr ratio free of cosmogenic contributions, we find a Martian mantle ^{86}Kr/^{84}Kr ratio of 0.3085 ± 0.0006 (1σ), same as the chondritic value (Table S1). The AVCC value seems a better match to the Martian mantle composition than Phase Q - a carbonaceous phase that carries the majority of heavy noble gases in chondrites and sometimes appears as the only trapped composition in achondrites (carbonaceous chondrites have additional presolar components) (*21*). However, we cannot rule out a mixture of Phase Q gases with a small amount of solar gases to match the observed ^{86}Kr/^{84}Kr value. The similarity of the Mars mantle ^{86}Kr/^{84}Kr ratio to chondritic Kr cannot result from addition of fission-produced Kr to solar or cometary Kr (*13*). Previous Kr measurements of Chassigny (Fig. 1) precluded accurate determination of the Martian mantle composition as these data either have large uncertainties (*14*, *16*) or consist of a single bulk measurement not targeted to determine the Martian interior composition (*22*). The ^{86}Kr/^{84}Kr ratio we infer for the Mars' interior is closest to AVCC, so we conclude that chondritic gases were incorporated into Mars' interior.

Chondritic noble gas ratios in Mars' interior are consistent with the observed elemental abundance ratios, ^{36}Ar/^{132}Xe and ^{84}Kr/^{132}Xe (Fig. 3), which are close to AVCC (*13*) and Phase Q (*21*) values, as previously demonstrated (*14*, *15*). Elemental ratios can be modified by magma degassing and gas extraction in the laboratory (*15*), leading to variations in Fig. 3. However, all data points are close to the chondritic value and are distinct from the solar, Mars atmosphere and Earth atmosphere.

Our xenon measurements are consistent with chondritic gases in Mars' interior. The $^{136}Xe/^{130}Xe$ ratio in Chassigny is distinct from the solar composition but close to the chondritic value, and consistent with a single mixing line (Fig. 2). Extrapolating to an AVCC $^{126}Xe/^{130}Xe$ ratio of 0.0255 (*13*) yields a Mars mantle $^{136}Xe/^{130}Xe$ ratio of 1.933 ± 0.022 (1σ). However, as discussed before, xenon isotopic compositions are more difficult to interpret due to multiple components and cosmic ray contributions for Xe are harder to correct for (*13*). Nonetheless, our Xe data are consistent with a chondritic component, though do not require it without incorporating the constraints from Kr.

Chondritic Kr and Xe in the Martian interior do not preclude acquisition of other volatile species from the solar nebula. For example, the $^{15}N/^{14}N$ ratio of Chassigny could reflect solar-derived N, although enstatite chondrites might also be the source (*15*). Objects larger than a lunar mass can gravitationally capture an atmosphere from the solar nebula, which might then be incorporated into the solid body (*1*). Although a minor solar component cannot be ruled out, the lack of detectable solar Kr in Chassigny precludes incorporation of large amounts of solar Kr into Mars' interior, either through magma oceans or through adsorption and burial beneath the surface during accretion (e.g., *1*).

Chondritic Kr in the Martian mantle contrasts with solar Kr in Mars' atmosphere (*17*, *18*). Cometary Kr, being depleted in ^{83}Kr and ^{86}Kr relative to solar (*23*), cannot account for the atmosphere Kr, suggesting atmospheric Kr was acquired from the solar nebula. Acquisition of the atmosphere from the solar nebula occurred after the interior incorporated chondritic Kr, as otherwise chondritic Kr signatures would be seen in the atmosphere. Both interior and atmospheric gases were accreted before the nebular gas dissipated on a timescale of ~4 Myr (*24*) due to radiation from the early Sun. Hence, Mars formed quickly, prior to complete nebular dissipation, accreting most of its mass and the solar atmosphere within 4 Myr after Solar System birth (*12*, *25*) (Fig. 4). The sequence of volatile accretion on Mars, chondritic followed by nebular, as suggested by our data, is opposite to most models of planet formation where chondritic volatile delivery follows solar gas acquisition (*1*).

The compositional differences between interior and atmosphere indicate that Mars' atmosphere was not generated primarily through outgassing from its interior, as often assumed (*26*). Because Mars' interior is enriched in heavier Kr isotopes compared to the atmosphere, outgassing followed by hydrodynamic loss is ruled out as that would leave the atmosphere enriched in heavier isotopes compared to the mantle. Delivery of chondritic volatiles to Mars' surface after dissipation of the nebula was probably limited because it would have left a mixture of solar and chondritic signatures in the atmosphere. Although planetesimal impacts would contribute to the budget of rare non-volatile elements (e.g., platinum group elements), that might not contribute substantially to Mars' volatile budget, particularly if the planetesimals are volatile-poor. Instead, planetesimal impacts may erode the atmosphere without inducing an isotopic fractionation, leading to net volatile loss (*27*).

A purely solar-like atmosphere would not persist on Mars if global magma ocean episodes persisted well past timescales of nebular dissipation, and/or if there were episodes of hydrodynamic escape due to higher solar activity (*26*, *28*). A magma ocean would outgas, causing interior-atmosphere exchange, while hydrodynamic escape would cause the atmosphere to be lost or heavily fractionated (*26*, *28*). Mass fractionation of Xe from a solar precursor recorded in the Martian atmosphere (*17*) might not be due to early hydrodynamic escape of neutral Xe, as Xe is the only noble gas that could escape as an ion, in a photo-ionized hydrogen wind. This process has been invoked to explain the prolonged Xe loss, but not other noble gases, in the Neoarchean era on Earth (*29*). Hence, Kr might be a better tracer of early atmospheric origin because it has kept its primordial solar signature. Gases lighter than Kr are lost from the modern Martian atmosphere in a mass-dependent fractionation process due to solar wind bombardment (*30*).

If Mars captured its solar-like atmosphere from the nebula, rather than acquiring it from mantle outgassing, it must have retained the solar-composition Kr-Xe after the nebula dissipated. Thus, magma ocean phases on Mars ended prior to complete nebular dissipation, consistent with rapid mantle solidification in about 4-5 Myr (*28*, *31*). Hydrodynamic escape of the solar-like atmosphere is expected to be an efficient process on Mars following nebular dissipation (*26*, *28*). To prevent loss of the solar-composition Kr-Xe during hydrodynamic escape, these gases might have been trapped in ice, either in the sub-surface or in the polar ice caps (*32*). However, this scenario would require Mars' surface to have remained cold, below the freezing-point of water after nebula dissipation. Later planetesimal impacts, or episodic periods of warmth, would have released the trapped Kr-Xe into the atmosphere. Occurrences of large-scale energetic events, such as magma ocean inducing large impacts, after accretion of the interior and surface volatiles, would be problematic as those would have mixed the two reservoirs.

Our study shows that within 4 Myr of Solar System formation, chondritic volatiles were incorporated into Mars' interior in large quantities; heavy noble gases reach abundances up to two orders of magnitude higher than in Earth's bulk mantle (*13*). The delivery of these chondritic volatiles to the inner Solar System may have been from material similar to enstatite chondrites (*6*), or from outer Solar System material scattered inwards by giant planet migration (*33*).

References and Notes

1. R. O. Pepin, D. Porcelli, *Rev. Mineral. Geochemistry*. **47**, 191–246 (2002).
2. M. W. Broadley *et al.*, *Proc. Natl. Acad. Sci.*, 202003907 (2020).
3. B. Marty, *Earth Planet. Sci. Lett.* **313--314**, 56–66 (2012).
4. S. Péron, S. Mukhopadhyay, M. D. Kurz, D. W. Graham, *Nature*. **600**, 462–467 (2021).
5. F. Albarède, *Nature*. **461**, 1227–1233 (2009).
6. L. Piani *et al.*, *Science.* **369**, 1110–1113 (2020).
7. C. M. O. Alexander *et al.*, *Science.* **337**, 721–723 (2012).
8. B. Marty *et al.*, *Science.* **356**, 1069–1072 (2017).
9. G. Holland, M. Cassidy, C. J. Ballentine, *Science.* **326**, 1522–1525 (2009).
10. S. Péron, M. Moreira, *Geochemical Perspect. Lett.* **9**, 21–25 (2018).
11. C. L. Harper, S. B. Jacobsen, *Science.* **273**, 1814–1818 (1996).
12. N. Dauphas, A. Pourmand, *Nature*. **473**, 489 (2011).
13. Materials and methods are available as supplementary material.
14. U. Ott, *Geochim. Cosmochim. Acta*. **52**, 1937–1948 (1988).
15. K. J. Mathew, K. Marti, *J. Geophys. Res.* **106**, 1401–1422 (2001).

16. U. Ott, T. D. Swindle, S. P. Schwenzer, in *Volatiles in the Martian Crust*, J. Filiberto, S. P. Schwenzer, Eds. (Elsevier, 2019), pp. 35–70.
17. P. G. Conrad *et al.*, *Earth Planet. Sci. Lett.* **454**, 1–9 (2016).
18. T. D. Swindle, *Rev. Mineral. geochemistry*. **47**, 171–190 (2002).
19. M. Moreira, *Geochemical Perspect.* **2**, 229–403 (2013).
20. A. Meshik, C. Hohenberg, O. Pravdivtseva, D. Burnett, *Geochim. Cosmochim. Acta*. **127**, 326–347 (2014).
21. H. Busemann, H. Baur, R. Wieler, *Meteorit. Planet. Sci.* **35**, 949–973 (2000).
22. O. Eugster, H. Busemann, S. Lorenzetti, D. Terribilini, *Meteor. Planet. Sci.* **37**, 1345–1360 (2002).
23. M. Rubin *et al.*, *Sci. Adv.* **4**, eaar6297 (2018).
24. H. Wang *et al.*, *Science.* **355**, 623–627 (2017).
25. R. Morishima, G. J. Golabek, H. Samuel, *Earth Planet. Sci. Lett.* **366**, 6–16 (2013).
26. H. Lammer *et al.*, *Astron. Astrophys. Rev.* **26**, 2 (2018).
27. H. E. Schlichting, S. Mukhopadhyay, *Space Sci. Rev.* **214**, 34 (2018).
28. N. V Erkaev *et al.*, *Planet. Space Sci.* **98**, 106–119 (2014).
29. K. J. Zahnle, M. Gacesa, D. C. Catling, *Geochim. Cosmochim. Acta*. **244**, 56–85 (2019).
30. B. M. Jakosky *et al.*, *Science.* **355**, 1408 (2017).
31. L. T. Elkins-Tanton, *Earth Planet. Sci. Lett.* **271**, 181–191 (2008).
32. K. J. Zahnle, *J. Geophys. Res. Planets*. **98**, 10899–10913 (1993).
33. D. P. O'Brien, K. J. Walsh, A. Morbidelli, S. N. Raymond, A. M. Mandell, *Icarus*. **239**, 74–84 (2014).
34. W. S. Cassata, *Earth Planet. Sci. Lett.* **479**, 322–329 (2017).
35. R. O. Pepin, L. E. Nyquist, D. Phinney, D. C. Black, *Geochim. Cosmochim. Acta Suppl. Proc. Apollo 11 Lunar Sci. Conf. Ed. by A. A. Levinson. New York Pergammon Press*. **2**, 1435–1454 (1970).
36. C. M. Hohenberg, P. K. Davis, W. A. Kaiser, R. S. Lewis, J. H. Reynolds, *Geochim. Cosmochim. Acta Suppl. Proc. Apollo 11 Lunar Sci. Conf. Ed. by A. A. Levinson. New York Pergammon Press*. **2** (1970).
37. S. Péron, S. Mukhopadhyay, M. Huh, *J. Anal. At. Spectrom.* (2020), doi:10.1039/D0JA00052C.
38. R. Wieler, *Rev. Mineral. Geochemistry*. **47**, 125–170 (2002).
39. U. Ott, *Chemie der Erde - Geochemistry*. **74**, 519–544 (2014).
40. M. Ozima, F. A. Podosek, *Noble Gas Geochemistry* (Cambridge University Press, 2002).
41. G. J. Taylor, *Geochemistry*. **73**, 401–420 (2013).
42. I. Azbel, I. N. Tolstikhin, *Meteoritics*. **28**, 609–621 (1993).
43. B. Marty, K. Marti, *Earth Planet. Sci. Lett.* **196**, 251–263 (2002).
44. A. N. Halliday, *Geochim. Cosmochim. Acta*. **105**, 146–171 (2013).
45. M. S. Lancet, K. Lancet, *Meteoritics*. **6**, 81–85 (1971).
46. L. C. Bouvier *et al.*, *Nature*. **558**, 586–589 (2018).
47. M. Grott *et al.*, *Space Sci. Rev.* **174**, 49–111 (2013).
48. O. Eugster, P. Eberhardt, J. Geiss, *Earth Planet. Sci. Lett.* **3**, 249–257 (1967).
49. K. Marti, *Earth Planet. Sci. Lett.* **3**, 243–248 (1967).
50. O. K. Manuel, R. J. Wright, D. K. Miller, P. K. Kuroda, *J. Geophys. Res.* **75**, 5693–5701

(1970).
51. D. Krummenacher, C. M. Merrihue, R. O. Pepin, J. H. Reynolds, *Geochim. Cosmochim. Acta*. **26**, 231–249 (1962).
52. J. J. Barnes *et al.*, *Nat. Geosci.* **13**, 260–264 (2020).
53. R. J. Floran *et al.*, *Geochim. Cosmochim. Acta*. **42**, 1213–1229 (1978).
54. A. Udry *et al.*, *J. Geophys. Res. Planets*. **125,** e2020JE006523 (2020).
55. F. M. McCubbin *et al.*, *Meteorit. Planet. Sci.* **51**, 2036–2060 (2016).
56. J. Filiberto, F. M. McCubbin, G. J. Taylor, J. Filiberto, S. P. B. T.-V. in the M. C. Schwenzer, Eds. (Elsevier, 2019), pp. 13–33.
57. G. Avice *et al.*, *Geochim. Cosmochim. Acta*. **232**, 82–100 (2018).
58. C. M. Hohenberg, B. Hudson, B. M. Kennedy, F. A. Podosek, *Geochim. Cosmochim. Acta*. **45**, 1909–1915 (1981).
59. J. R. Basford, J. C. Dragon, R. O. Pepin, M. R. Coscio Jr., V. R. Murthy, in *Lunar and Planetary Science Conference Proceedings* (1973), vol. 4 of *Lunar and Planetary Science Conference Proceedings*, pp. 1915–1955.
60. T. D. Swindle, M. W. Caffee, C. M. Hohenberg, *Geochim. Cosmochim. Acta*. **50**, 1001–1015 (1986).
61. R. O. Pepin, *Space Sci. Rev.* **92**, 371–395 (2000).
62. K. J. Mathew, J. S. Kim, K. Marti, *Meteorit. Planet. Sci.* **33**, 655–664 (1998).
63. K. Marti, P. Eberhardt, J. Geiss, *Zeitschrift für Naturforsch. A*. **21**, 398–426 (1966).
64. P. Eberhardt, E. Eugster, K. Marti, *Z. Naturforsch.* **20a**, 623–624 (1965).
65. A. O. Nier, *Phys. Rev.* **77**, 789–793 (1950).
66. Y. Sano, B. Marty, P. Burnard, in *The Noble Gases as Geochemical Tracers*, P. Burnard, Ed. (Springer Berlin Heidelberg, 2013), *Advances in Isotope Geochemistry*, pp. 17–31.
67. V. S. Heber *et al.*, *Geochim. Cosmochim. Acta*. **73**, 7414–7432 (2009).
68. E. Mazor, D. Heymann, E. Anders, *Geochim. Cosmochim. Acta*. **34**, 781–824 (1970).
69. D. D. Bogard, D. H. Garrison, *Geochim. Cosmochim. Acta*. **62**, 1829–1835 (1998).

Acknowledgements: We thank Rainer Wieler and two other anonymous reviewers for comments that greatly improved the manuscript. We thank the French National Museum of Natural History (MNHN, Paris, France) for graciously providing the Chassigny meteorite samples. We also thank Dylan Spaulding for assistance in preparing the samples. Magdalena Huyskens, Philip J. Carter and Sarah Stewart are thanked for fruitful discussions and comments.

Funding: Funds provided by University of California, Davis to S.M.

Author contributions: S.P. and S.M. both designed the study, performed the noble gas analyses, interpreted the results and wrote the manuscript.

Competing interests: We declare no competing interests.

Data and materials availability: Our samples of Chassigny were obtained from MNHN, numbers 2525 PE2 & PE3. The samples were consumed during the experiments. Our noble gas (neon, argon, krypton, xenon) measurements are reported in Tables S1 to S3.

Supplementary Materials

Materials and Methods
Supplementary Text
Figs. S1 to S4
Tables S1 to S4
References (34 - 69)

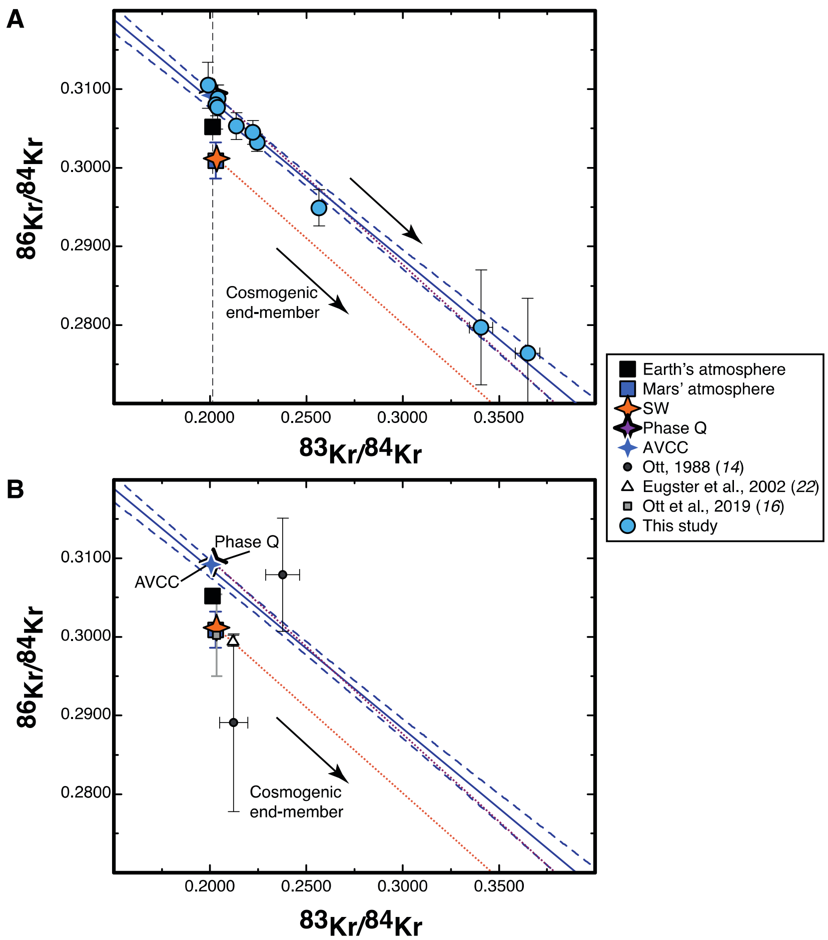

Fig. 1. Krypton isotopic composition of Chassigny. A) Our measurements of Chassigny are shown as blue circles with the data points representing the different temperature steps (the first four steps are not shown in the figures). The compositions of Phase Q (*21*), average carbonaceous chondrites (AVCC) (*13*), solar wind (SW) (*20*), Earth's atmosphere and Mars' atmosphere are shown with symbols indicated in the legend. The blue line is a linear model fitted to the Chassigny data, with the 95% confidence interval as dashed lines. The dotted lines indicate values obtained by mixing Phase Q (purple)/solar wind (orange) with cosmogenic krypton (*13*). The vertical dashed line indicates the $^{83}Kr/^{84}Kr$ ratio free of cosmogenic contributions (*13*). B) Same data as panel A, but compared to previous measurements of Chassigny (*14*, *16*, *22*). In both panels, errors bars indicate 1σ uncertainties. Fig. S1 shows additional details and isotope ratios.

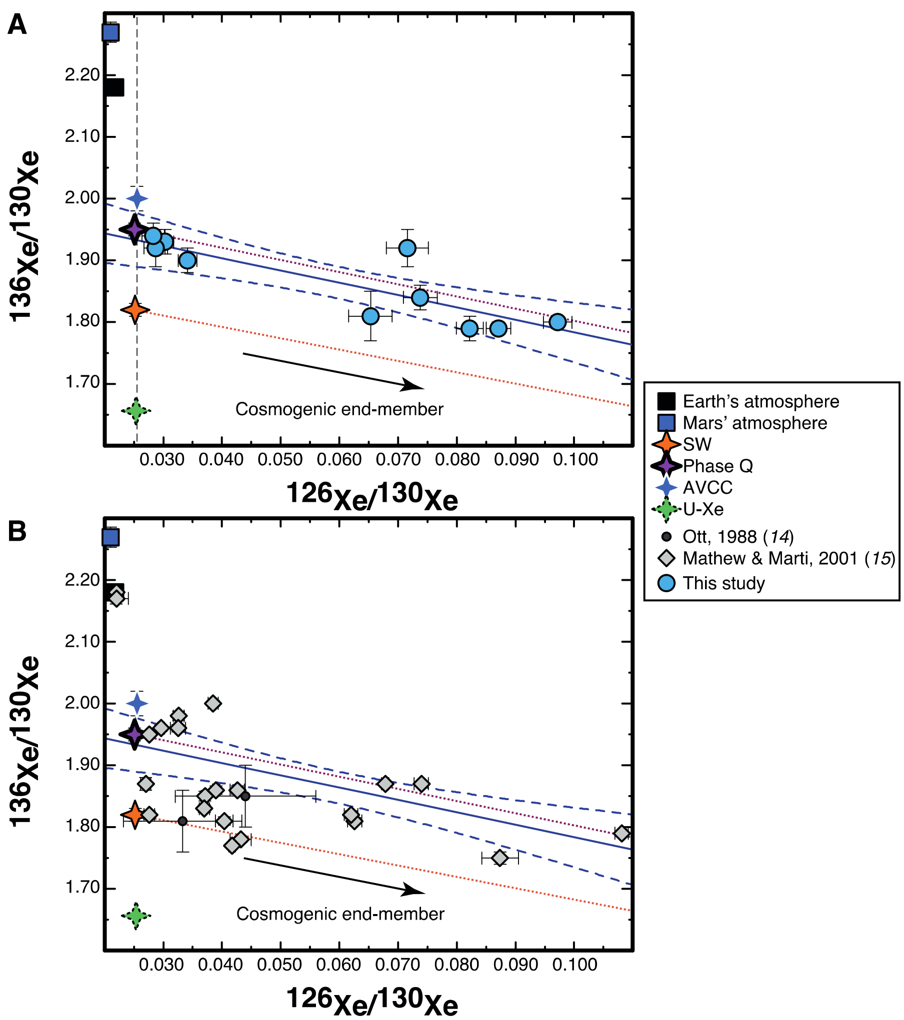

Fig. 2. Xenon isotopic composition of Chassigny. A) and B) Same as Fig. 1 but for xenon. Also shown is the U-Xe value, thought to be the Earth's atmosphere precursor (*1*), a mix of about 80% chondritic Xe with 20% cometary Xe (*8*).

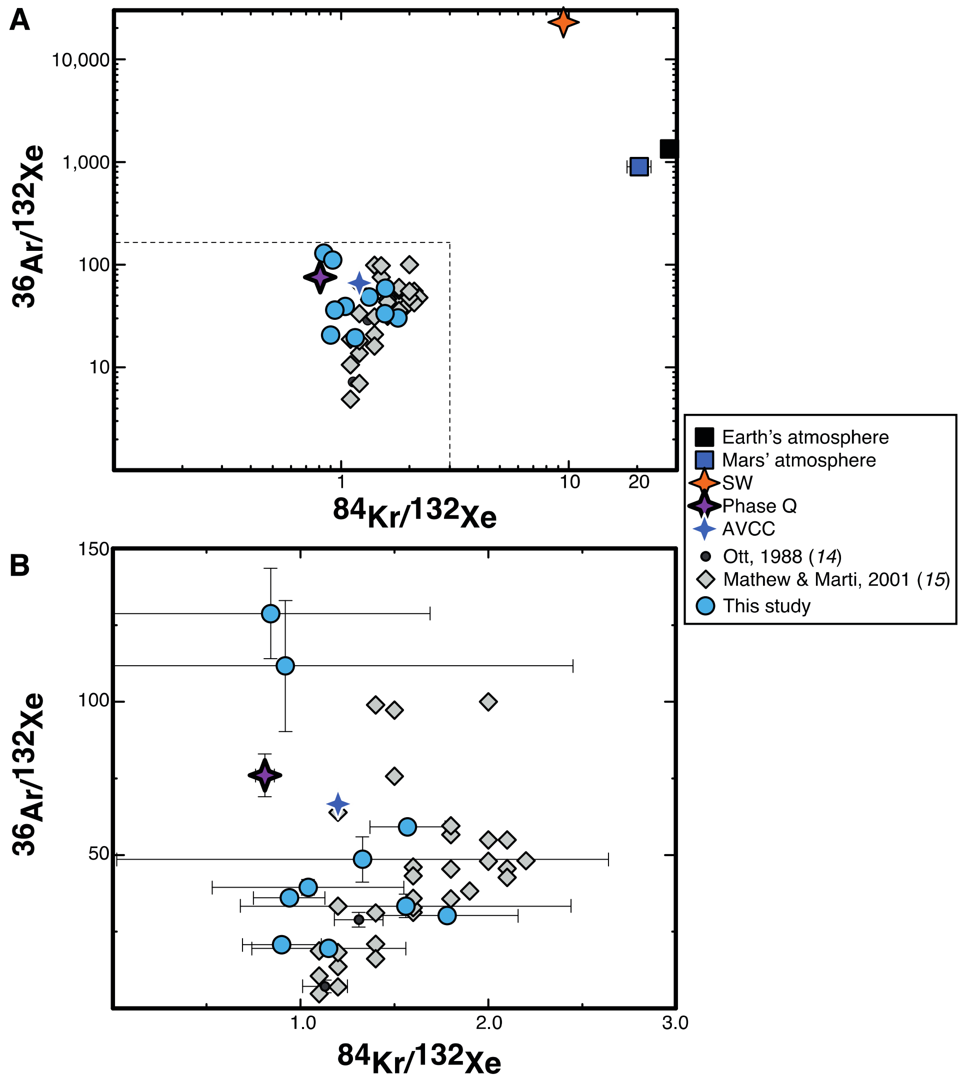

Fig. 3. Heavy noble gas abundances measured in Chassigny, after correction for cosmogenic contributions. A) Argon, krypton and xenon elemental ratios for our measurements of Chassigny in the different temperature steps. For comparison, we show previous measurements of Chassigny (*14*, *15*), solar wind, Phase Q, average carbonaceous chondrites, Earth's atmosphere and Martian atmosphere (references in Table S4). B) Close up of region within the dotted box in panel A.

Errors bars show 1σ uncertainties and are smaller than symbol size for solar wind and Earth's atmosphere.

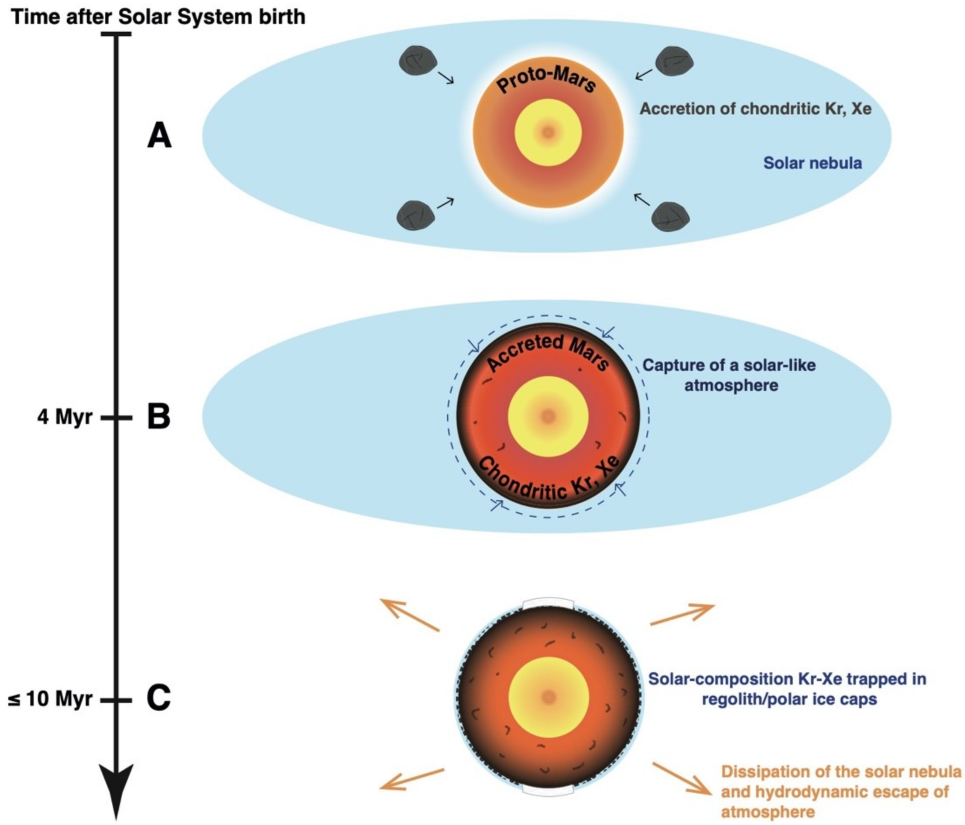

Fig. 4. Diagram illustrating a possible scenario for volatile delivery to Mars. A) Accretion of chondritic Kr and Xe from planetesimals (grey), forming Mars' mantle (orange) and core (yellow). This occurs within the gaseous solar nebula (blue) during the first Myr of Solar System formation. A magma ocean might have existed at this stage with either no, or a thin tenuous atmosphere (white grading into blue solar nebula). B) After most of Mars' mass accreted (~ 4 Myr after Solar System birth (*12*)) and a solid lid formed at the surface, an atmosphere with solar isotope ratios is gravitationally captured (dashed blue circle). The atmosphere may not have been massive such that solar-composition gases were not incorporated into the interior in substantial quantities. C) The surrounding nebula dissipates, halting accretion of solar-composition gases to atmospheric and surface reservoirs. Limited exchanges occur between the heterogeneous mantle and the atmosphere. Atmospheric solar-composition Kr and Xe may have been trapped in polar

ice caps (white) and/or in the sub-surface to prevent its loss during hydrodynamic escape of the atmosphere.